

Review article

RECENT IMPROVEMENTS OF THE OPTICAL AND THERMAL PERFORMANCE OF THE PARABOLIC TROUGH SOLAR COLLECTOR SYSTEMS

Asaad Yasseen Al-Rabeeh^{1,3}, István Seres², István Farkas²

¹Doctoral School of Mechanical Engineering, Szent István University, Hungary

²Department of Physics and Process Control, Szent István University, Hungary

³Department of Mechanical Engineering, Faculty of Engineering,
University of Kufa, Iraq

Abstract. *Parabolic trough solar collectors (PTSCs) are commonly used for applications that reach a temperature of up to 500 °C. Recently, improving the efficiency of PTSCs has been the focus of research because PTSCs have advantages, such as cost and size reduction and improved optical and thermal performance. This study summarizes relevant published research on the preparation, properties and experimental behavior of the optical and thermal properties of PTSCs. Analyzing of the thermal modeling method presents a steady and transient heat transfer analysis. Optical efficiency depends on material properties, such as mirror reflectance, glass cover transmittance, receiver absorption–emission, intercept factor, geometry factor and incidence angle. Also analyzed and discussed are the models used in computational fluid dynamics to study the physical properties of PTSCs. Lastly, studies on PTSC performance and enhancement, including novel designs, enhancement of passive heat transfer and laden flows of nanoparticles inside the absorber tube, are presented and examined separately. Nanofluids have illustrated their advantages and ability to increase heat transfer rates. Moreover, other works that aimed to enhance the optical and thermal efficiency of PTSCs are evaluated.*

Key Words: *Parabolic Trough Solar Collector, Optical Analysis, Heat Transfer Enhancement, Simulation Tool Analysis, Nanofluid*

Received November 06, 2020 / Accepted March 11, 2021

Corresponding author: Asaad Y. Al-Rabeeh

Mechanical Engineering, Szent István University, Páter Károly utca 1., Gödöllő, H-2100, Hungary.

E-mail: asaady.hussein@uokufa.edu.iq

1. INTRODUCTION

The global energy demand is continuously increasing with the depletion of the conventional energy sources. Solar energy is a usable and clean renewable energy source which is used as an alternative for producing energy from fossil fuels. Solar radiation is reflected, diffused or absorbed by solid particles, especially by the earth's surface, depending on many factors, such as climate, weather, agriculture and the earth's geometry [1, 2]. The parabolic trough solar collector (PTSC) technology is one of the most reliable technologies in the field of solar thermal [3]. It is mainly used for power generation (e.g. generating steam which needs high temperature) and other technological purposes [4, 5]. In the case of PTSCs, thermal energy is collected from solar radiation in the focal point of a special geometry to reach a high temperature [6]. The collectors receive direct solar radiation from the sun over a large surface and gather it to the focal point. A fluid flowing inside the tube absorbs the heat energy generated from the focused solar radiation, raising its enthalpy and causing an increase in the temperature of the tube wall [7, 8]. PTSC is an active technology used in the field of solar thermal applications. It consists of a reflecting surface, an absorber tube and the working fluid passing through the tube [9]. The design should be accurate to increase thermal efficiency, and the material of low weight, high mechanical strength and high thermal conductivity is preferable [10, 11]. The thermal conductivity of the absorber tube material affects the performance of PTSCs by increasing the heat transfer between the working fluid and the metal [12, 13]. A working fluid is an essential component for enhancing the efficiency of PTSCs. The mixing of nanoparticles with the working fluid is an effective method of increasing the collected thermal energy and the nanofluids' thermophysical properties, such as enthalpy, specific heat capacity, thermal conductivity and density [14, 15]. The thermal efficiency of PTSC depends on the concentration of the volume fraction of nanoparticles in the base fluid [16].

This study primarily aims at summarizing the key advances made in PTSCs and identifying the factors to take into consideration in future developments. Continuing research and development activities have helped this PTSC technology become the most economically and technologically advanced of all current concentrating solar power technologies. This thorough analysis is conducted in order to study different modeling research and methods used to simulate PTSCs. Detailed reviews of theoretical studies on thermal and optical performance are performed. Moreover, studies on performance improvement techniques and dealing with the alteration of the design of PTSCs are evaluated. For increasing heat transfer is the insertion of tabulators in the PTSCs design while the use of mono and hybrid nanofluids is to improve efficiency and thus the performance of PTSCs.

2. PTSC SYSTEM

2.1. Background

In 1883, Captain John Ericsson used a parabolic trough concentrator (PTC) to work on solar-powered machines for irrigation. However, his experiment on solar engines did not advance to the prototype stage. The invention of the parabolic trough is essential. In 1912, a 45-kW power plant was built in Egypt. The system was composed of five solar collectors and was oriented north-south with a system of mechanical tracking [17]. The system generated steam that was used to operate water pumps for irrigation. The

development of the parabolic trough power occurred in the US in the 1970s and in Europe in the 1980s [18]. PTSCs could produce high temperatures (above 500 °C) to produce industrial process heat. The development was sponsored or conducted by the Sandia National Laboratories in New Mexico. In 1981, the International Energy Agency developed a small solar power system in Tabernas, Spain. In 1982, Luz International Limited (Luz) advanced a parabolic trough collector. In 1985, Luz built eight power plants of PTSCs in California, US. Today, according to the database of the National Renewable Energy Laboratory, over 97 plants are at different stages of development of this parabolic trough-based technology. The design of these power plants is to produce electrical power from steam obtained from natural gases or solar fields. The parabolic trough power plants of Nevada Solar in the US produce 72 MW capacities, and the Martin Solar Plant Centre has 75 MW net capacities. The Andosol plant is the first parabolic trough power plant in Spain. Many plants in Spain have similar operational characteristics (e.g. Andosol with 50 MW and 7.5 h storage energy), some are under construction (e.g. Vallesol 50 with 50 MW and 7.5 h storage energy) [19]. The scholars are still trying to improve and increase the parabolic trough power plants efficiency.

2.2. PTSC Systems Fundamentals

A PTSC system is a technology that concentrates solar energy in a focal line to convert it into thermal energy of the high-temperature medium. It can obtain temperatures of up to 500 °C, depending on the application [20]. A mathematical model of the parabola, in terms of the coordinate system, is shown in Fig. 1.

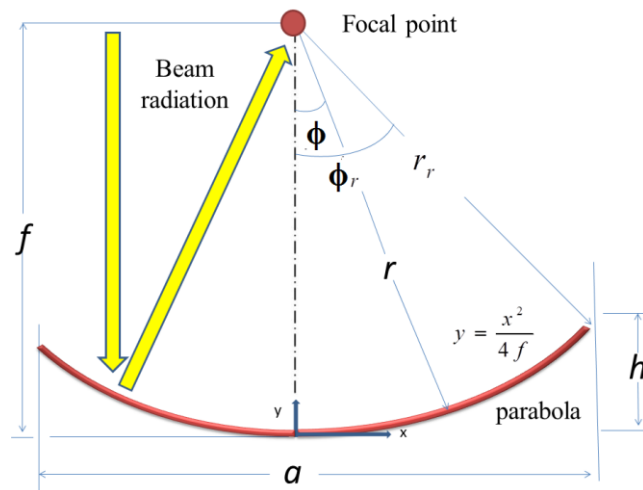


Fig. 1 Parabolic concentrator [21]

In Fig. 1, $y = x^2/4f$ represents the parabola equation, a - the aperture, f - focal distance, h - depth, r - the rim radius, ϕ - the rim angle, r_r - the rim radius when the angle $\phi = \phi_r$.

The collector receives the direct solar radiation from the sun over a large surface and focuses on it. The PTSC has a curved reflector or a parabolic mirror for reflecting and

concentrating the solar radiation onto specific points or a line. The mirror is manufactured from different materials to reduce absorption losses, such as low iron glass or aluminum. Many factors are important in the production of collector mirrors; these factors include solar-weighted reflectivity, durability, abrading properties and cost. The gluing, silvering and protective coating processes are performed after bending the mirror [22]. The heat collection element (HCE), also referred to as the receiver, is placed at the focal axis. The heat transfer fluid circulates through the absorber.

A fluid flowing inside the tube that absorbs the heat energy generated from the focused solar radiation raises its enthalpy and causes an increase in the temperature of the tube wall. PTCs can be used only in direct solar radiation in the collectors, which are not deviated by dust, fumes or clouds. The absorber tube should be coated by a material of the antireflective layer to minimize the heat losses generated by radiation [23]. The effectiveness of the solar thermal collector is calculated by measuring the fluid temperature difference between the inlet and the outlet and by the flow rate of the working fluid [24].

2.3. Modeling and Simulation of PTSCs

The progress of computing has helped researchers in analyzing the system by modeling and simulation. Engineering programs can be used to study the system performance and the effect of several variables with minimum time and low cost [25]. Recently, many modeling studies have been performed and have facilitated the development of PTSCs; these studies involved thermal and optical analyses through the modeling and simulation of PTSCs. By modeling the system, the factors can be analyzed and handled separately (e.g. temperature and the properties of optical materials) [26]. The modeling and simulation of PTSCs can be covered as depicted.

3. PTSC-SYSTEM OPTICAL ANALYSIS

Optical efficiency η_o can be obtained by the rate of energy absorbed from radiation in the absorber tube and the amount of the energy incident on the aperture of the collector.

$$\eta_o(\theta = 0) = \rho \tau \alpha \gamma, \quad (1)$$

where: ρ - the mirror reflectivity, τ - the glass envelope transmittance, α - the absorptivity of surface coating, γ - the mirror interception factor, θ - the incidence angle.

The efficiency curves are generally calculated at normal incidence; however, the incidence angle for the tracked collector at a single axis changes during the operation. The optical efficiency of PTSCs decreases with incidence angle for several reasons, including the increased width of the solar image on the receiver, the decreased transmission of the glazing, the absorption of the absorber and the spillover of the radiation from troughs of finite length. The effect of the angle of incidence must depend on the difference in all optical properties. It can be correlated by a modification called the change in the angle of incidence [27]. A method of reducing the end loss effect in a short trough collector is to recompense the length of the absorber tube [28].

A different way of calculating end loss is presented in cylindrical troughs. The optical design of PTSCs is influenced by several factors [29], including apparent changes in the incidence angle effect and the sun's width, mirror construction and the materials used in

the heat collector element, poor operation, incomplete tracking of the sun's rays and the manufacturing defects of the PTSC. The next two parts discuss the way in which the analytical and ray tracking approaches for optical errors are perceived and used in the study of PTSCs.

3.1. Optical Analysis of Errors

Optical performance is determined by using an analytical approach to obtain the closed intercept factor. A mathematical expression is determined for the intercept factor by Gaussian distribution [30]:

$$\gamma_{GUSS} = \int_{-\infty}^{\infty} d\theta f(C\theta) \frac{1}{\sigma_{tot} \sqrt{2}} \exp\left(-\frac{\theta^2}{2\sigma_{tot}^2}\right), \quad (2)$$

$$\sigma_{tot} = (\sigma_{sun}^2 + \sigma_{mirror}^2 + \sigma_{slop}^2 + \sigma_{tracking}^2 + \sigma_{displacement}^2)^{\frac{1}{2}}, \quad (3)$$

where: σ_{tot} - total optical error, σ_{sun} - beam intensity error, σ_{mirror} - surface mirror error, σ_{slop} - local slop error, $\sigma_{tracking}$ - tracking error, $\sigma_{displacement}$ - displacement error, C - concentration ratio.

Total optical error σ_{tot} is obtained from this approach by making all errors in a single term [31]. Two groups of optical errors, namely, random and nonrandom, are shown in Fig. 2.

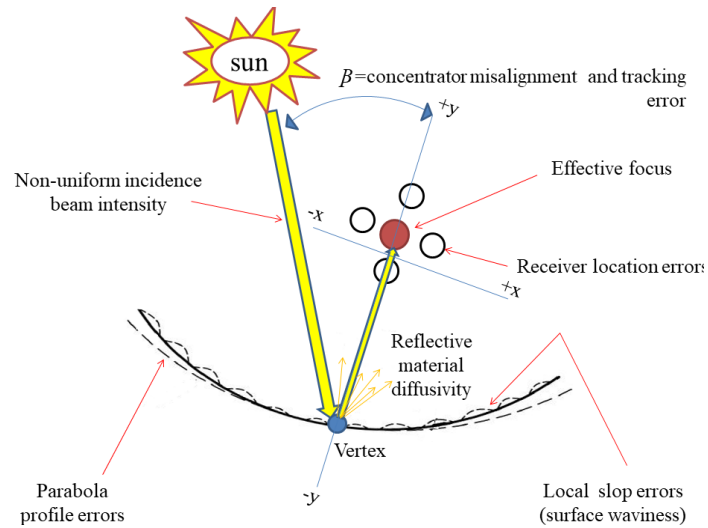


Fig. 2 Potential optical error description in PTSCs [4]

The intercept factor can be obtained from [32]

$$\gamma = \frac{1 + \cos\phi_r}{2 \sin\phi_r} \int_0^{\phi_r} \left[\frac{\operatorname{Erf} \left[\frac{\sin\phi_r(1 + \cos\phi)(1 - d^* \sin\phi) - \pi(1 + \cos\phi_r)}{\sqrt{2\pi\sigma^*}(1 + \cos\phi_r)} \right]}{\operatorname{Erf} \left[\frac{\sin\phi_r(1 + \cos\phi)(1 - d^* \sin\phi) - \pi\beta^*(1 + \cos\phi_r)}{\sqrt{2\pi\sigma^*}(1 + \cos\phi_r)} \right]} \right] \frac{d\phi}{(1 + \cos\phi)}, \quad (4)$$

where: E - total energy, d^* - the universal nonrandom error parameter due to HCE dislocation and mirror profile errors; β^* - the universal nonrandom error parameter due to angular errors; σ^* - the universal random error parameter.

3.2. Ray Tracing

The ray-tracing technique is used for analyzing the optical and optical design/optimization performance of PTSCs. It benefits the systems that contain many surfaces and Newtonian imaging equations and those in which the Gaussian is inappropriate. Ray tracing supplies a massive amount of detailed information for the optical characteristics of the system [33]. Computer technology helps reduce the time for optical analyses. Software tools that use the ray tracing technology include Optical, ASAP, TracePro, SolTrace and SimulTrough, using the Monte Carlo ray tracing (MCRT) method in the optical analysis of a PTSCs [34].

4. HEAT TRANSFER ELEMENT FOR PTSC

The heat transfer element in PTSCs is a major component and contains an absorber tube; it is an essential part that contributes to the proper performance of the system. Solar radiation is focused on the absorber tube, and a heat transfer fluid (e.g. thermal oil, water and nanoparticle-laden fluid) moves through the tube [21]. A schematic of a solar trough parabolic receiver is shown in Fig. 3.

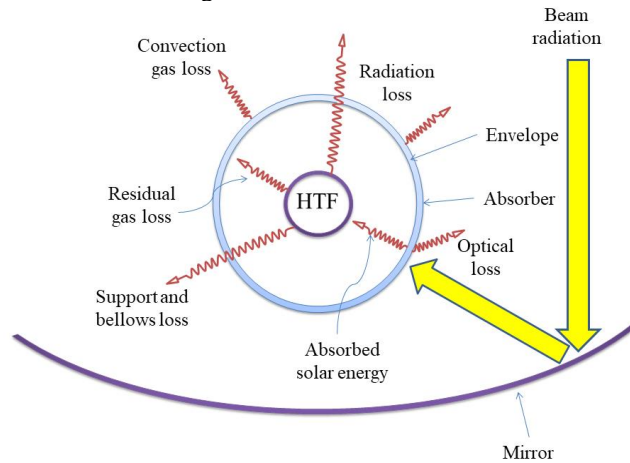


Fig. 3 The schematic figure of losses of the solar trough parabolic receiver [37]

The losses are indicated in the cross section of the tube. An evacuated glass envelope covers the absorber tube to reduce the heat losses. The fluid flow by forced convection in the absorber tube may be in single or two phases. In this case, the flow process in these systems, the heat transfer coefficients and the equation to the HCE modeling of heat transfer are much more complex [35, 36].

5. COMPUTATIONAL FLUID DYNAMICS (CFD) ANALYSIS

For the numerical modeling of the fluid flow (can be laminar or turbulent flow) inside the tube of PTSCs, computational fluid dynamics (CFD) is used to analyze the HCE's overall thermal hydraulic efficiency. The CFD modeling method includes continuity and momentum numerical solutions and energy balance equations. To predict PTSC output correctly during a CFD study, actual boundary conditions must be used. The key to these boundary conditions is the heat flux on the absorber tube of the HCE; in the study, this heat flux is typically the leading thermal boundary state [38]. Details of studies conducted with CFD are summarized in Table 1.

Table 1 Summary of traditional PTSC CFD-analysis

Ref.	Type of Study	Findings
[39]	Ansys	The difference in the heat flux has a major effect on deciding the overall circumferential HCE temperature. With an increase in the nonuniformity of HCE distribution, heat loss decreases. When the angle of the incidence decreases, so does heat loss. Therefore, the rate of heat loss gradually decreases in accordance with radius ratio (RR) (i.e. relationship between the inner radius and the outer radius of the absorber envelope), which decreases, thus reaching the minimum amount for RR=1,375 if the heat transferred starts after that critical value only through conduction and convection.
[40]	Fluent	The critical of RR is less for large-diameter absorber diameters. For a given HCE, the critical RR is independent of the HCE temperature and outer wind velocity in the weather. In the space of the nonevacuated HCE, the contrast of heat transfer losses in individual and variable temperature in a tube in the cases is 1.5%. The RR and wind speed in the evacuated HCE have marginal effects on the thermal losses.
[41]	Fluent	Rising heat transfer at high mass flow rates means the absorber outlet has a high capacity for thermal energy. As the losses in convection rise by wind speeds around the collector, the temperature in the outlet decreases. Therefore, the circumferential temperature gradient is nearly even for the absorber tube of copper material compared with one-steel material.
[42]	Fluent	The heat flux distribution becomes gentler as the concentration ratio increases, the angle span of the region decreases, and the absorber's shadow effect becomes less powerful. Increasing the concentration rate can also increase the HTF temperature. Increasing the angle of the rim reduces as much heat as possible. When the angle of the rim is small, the glass cover reflects many rays; the temperature elevation is much lower.
[43]	Fluent /MCRT-code	When the HTF is steam in different process settings, the thermal stress inside the tube is great. Moreover, highly effective solar radiation that focuses on the absorber tube and the high steam temperature contribute to high heat transfer gradients with comparable levels of steam mass flow.
[44]	Fluent	

[45]	Ansys Fluent /SolTrace	When the angle of rim increases, the gradient of the circumferential temperature on the surface of the absorber is reduced. The reduction in the peak temperature of the absorber is low as the angle of the rim is greater than 80°. Bejan number, a measure in which irreversibility between heat transfer and irreversibility in fluid friction is dominant. It also increases with a reduction of the rim angle and temperature of HTF and increase the ratio of concentration.
[46]	Ansys Fluent	The Nusselt number variance is smaller than that of the nonuniform heat transfer flux under uniform heat transfer flux. With the solar elevation angle, the resistance to flow increases. When the number of Grashof increases and the number of Nusselt increases rapidly with the angle of solar elevation then it starts to decrease slowly at the increase of higher Grashof numbers and low on the solar elevation angles.
[47]	MCRT-code/Ansys Fluent	Increased errors in tracking decrease the thermal efficiency. The thermal output drops from 70.64% to 9.41% by raising the error of tracking from 0 mrad to 20 mrad.

6. ENHANCEMENT OF OPTICAL EFFICIENCY

6.1. Selective Surface Coating on the Receiver Tube

Optical efficiency is calculated as the energy ratio of the absorbed energy to the energy incident received on the collector's aperture [48]. The coating changes have been improving HCE performance. The HCE output is prone to any difference in the optical properties of the selective coating. Many studies have been conducted to enhance absorption and reduce selective surface emission. The microstructure of the material is influenced by extremely high temperature [49]. The coatings should be structurally robust and suitable, safe to handle for extended periods, stable at operating temperatures, environmentally friendly and relatively inexpensive.

6.2. Antireflective Surface Coating on the Glass Tube

In solar applications, borosilicate glass tube should be installed around the absorber and should have high transmissometer properties. Selective surface coating on glass increases transmittance from approximately 92% to 96% [50].

6.3. Mirror Reflectivity

The reflective surfaces are coated by silver, and then followed by layers of copper to increase the quality of the highly polished reflectivity mirror surface 94.5%. The cleaning of mirrors is vital for the efficiency of the solar collector assembly [51].

6.4. Absorber Tube Intercept Factor

The intercept factor effects on optical efficiency are determined as part of the ray's incident angle upon the aperture that reaches the receiver for a given incidence angle. The intercept factor is the parameter that embodies the effect of errors. The local slope and profile errors occur during manufacture. Thomas developed a technique to measure the flux distribution around the receiver of PTCs. If the distribution of the flux around the absorber is known, then the intercept factor can be easily calculated [52].

6.5. Incorporating Secondary Reflectors

The essential primary concentrator reflects the solar radiation on the receiver tube either through a mirror or a polished aluminum sheet. The collector that intercepts the radiation flux depends on factors, such as primary focus surface error, rim angle and rigidity of the structure, to withstand wind and self-load and mechanism tracking accuracy. The spillage or dispersion of high-concentration radiation across the source creates a considerable optical and thus thermal efficiency loss [53].

6.6. Dual Axis Tracking and End Losses

The geometrical aspect of the collector determines the optical efficiency and performance, decrease of the opening area induced by the irregular effect, blocks, shadows and radiation loss beyond the receiving end. Radiation occurring on the concentrator's edge observe the solar radiation cannot enter the receiver tube that is called end effect. Xu conducted an optical study of the end loss effect and then proposed a mirror design to enhance thermal efficiency. The end loss effect is gradually reduced by increased trough length [54].

7. PERFORMANCE ENHANCEMENT TECHNIQUES

Many researchers have studied heat-transfer improvement techniques to enhance the thermal performance of PTSCs and thus increase their efficiency. PTSC systems can be improved by changing either their heat collector element properties or optical design. Various heat-transfer enhancement techniques have been used in PTSCs.

7.1. PTSC Receiver with Glass Envelope

The materials and dimension of the absorber tube affect the performance of PTSCs [55]. The performance of the collector increases with that of the glass cover tube. The glass cover tube reduces the convective heat losses and enhances the performance of the PTSC system by improving the greenhouse effect between the glass and the tube [56]. Having a top glass cover increases instant efficiency by 45.56%–62.60% and total efficiency by 10% [57]. Kasaeian et al. (2015) designed and manufactured a small prototype model of PTSCs to investigate the methods for enhancing the performance of PTCs. The system was compared with different receiver tubes to improve the optical, thermal and heat transfer of the PTSCs, with vacuumed steel tube with black paint, black chrome coating copper tube, copper-vacuumed black chrome coating and black chrome coating copper tube with nonevacuated glass cover tube. The test of the different receiver's tube used MWCNT/oil nanofluids in 0.2% and 0.3% volume fraction. The best results were obtained in the vacuumed receiver, and the efficiency improved by 11% higher than the nonevacuated tube. The maximum optical and thermal efficiency of the vacuum copper receiver system was found to be 61% and 68 %, respectively, due to a high absorption rate of 0.98% [58].

7.2. Novel Designs

The focus of the novel design focuses on enhancing optical efficiency by increasing the absorbed radiation or decreasing collector heat loss. Bader studied the heat transfer

analysis of the cylindrical air-based cavity-receiver tube. The receiver efficiency ranged from 45% to 29%. At summer solstice solar noon, the HTF inlet temperature was 120 °C, and the HTF outlet temperature ranged from 250 °C to 450 °C. The loss of solar radiation on the absorber tube is equal to one third by spillage [59]. The heat loss between two paired horizontal cylinder receivers was studied in conduction and convection in absorber tube from a half-isolated annulus. The application of fibreglass insulation to the half of the annulus away from the parabolic trough increases the reduction of convection heat losses by an average of approximately 25% relative to traditional receivers [60].

Demagh studied the possibility of establishing an S-curved/sinusoidal receiver tube in PTSCs. The PTSC was replaced with a traditional straight absorber, whose designed S-curved/sinusoidal and heat flux density distribution varies on the axial and the azimuthal directions. The heat flux density was distributed on a large surface [61]. Xiao designed a tube absorber by a V-cavity on PTSCs. The optical efficiency of the absorber improved with reduced aperture distance and increased depth-to-width ratio [62].

7.3. Improving Passive Heat Transfer

Many researchers studied the collector improvement by passive convective for increasing heat transfer in the absorber tube. Various inserts, such as regularly spaced, straight twisted, helically twisted and twisted perforated tapes; protrusion; dimples; wire loops; longitudinal strips; and insert butterfly strings, are used. The thermodynamic, fluid friction and heat transfer performance increase as the width ratio increases and the twist ratio decreases. A significant decrease in the generation of entropy is achieved at a low Reynolds number at the twist ratio and decreased the width ratios, while the ideal Reynolds number increases. A considerable increase in the heat transfer performance of about 169%, reduction in the absorber tube's circumferential temperature difference is up to 68% while increase in thermal efficiency is up to 10% over a receiver with a plain absorber tube [45].

Various porous receiver geometries have been considered for the performance estimate of PTSCs. Thermal analysis of the receiver tubes was performed for various geometric parameters, such as thickness and ratio of fin aspect and porosity, for varying heat flux conditions. The porous fins inserted into the tubular receiver of the STC enhanced the heat transfer compared with the solid longitudinal fins [63]. Porous circular, triangular, square and trapezoidal inserts and the heat losses in all porous inserts were found to be approximately the same [64].

Helical fins are utilized in internal tubes for the design of PTSCs. Many factors, such as thermal loss, pressure loss, thermal fatigue and thermomechanical stress, affect the performance of PTSCs [65]. The results show that the parasitic losses associated with the pressure losses in the tube increase with the number of fins and its helix angle. Although the thermal losses and temperature gradients are reduced, the energetic and thermal efficiency of the collector increases [66].

On the other hand, several drawbacks in this way, such as increased parasite loads associated with increased pressure loss, noise and additional manufacturing costs, exist.

7.4. Nanofluid

Nanofluid is a term used to describe a fluid in which nanometre-sized particles are suspended with normal scales of 1–100 nm in length [67]. Nanoparticles in liquids are suspended to improve thermal conductivity and heat transfer efficiency of basic liquids

[68]. The thermal conductivities of particulate content are typically higher in magnitude, particularly at low volume levels, compared with those of specific fluids, such as water, ethylene glycol and light oils and nanofluids [69].

They can dramatically improve the host fluid thermal efficiency and thermophysical characteristics of PTSCs [70, 71]. In the simulations, two major groups emerge: (1) the single-phase modeling that considers the mixture of nanoparticle and base fluid as a single-phase mixture with stable properties and (2) the two-phase modeling that considers the properties and behavior of the nanoparticle separately from that of the base fluid [72].

The pressure drop increases with an increasing volume concentration of nanoparticles in the base fluid. When the Reynolds number increases, the pressure drop increases sharply. The pressure drop is a function of the fluid's thermophysical properties and velocity of inlet fluid in the absorber tube [73]. The force of inter nanoparticles is highly influenced by the concentration of the nanoparticles. The force profiles are influenced by many factors, such as time, size, shape, surfactant concentration and humidity. In greater concentrations nanoparticles increasingly begin to accumulate, swarm, precipitate out of the solution, and adsorb on surfaces [74]. For example, synthetic oils have a temperature of >400 °C, whereas molten salts reach up to 600 °C. By contrast, it is anti-freezing systems due their temperature of solidification about 220 °C [75].

7.4.1. Mono nanofluids

A single kind of nanoparticle is suspended with a fluid. In a study, the modeling and simulation of synthesized nanofluids should predict the thermophysical properties to ensure acceptable results. The thermophysical properties for any nanoparticle and fluid become new properties of density, viscosity, specific heat capacity and thermal conductivity [76].

Three main parameters involved in calculating the heat transfer rate of the nanofluid are heat capacity, viscosity and thermal conductivity, which may differ from those of the original pure fluid. The density and specific heat of the dispersed liquid are homogenous, and the thermodynamically stable state [77] could be determined from

$$\rho_{nf} = \rho_f (1 - \phi) + \rho_p \phi, \quad (5)$$

where: ρ_{nf} - nanofluid density, ρ_f - fluid density, ρ_p - particle density, ϕ - the volume fraction of the nanoparticles.

Furthermore, the specific heat based on the heat capacity concept is as follows [78]:

$$c_{p,nf} = \frac{\rho_{nf} c_{p,f} (1 - \phi) + \rho_p c_{p,p} \phi}{\rho_{nf}}, \quad (6)$$

where: $c_{p,nf}$ - the specific heat capacity of nanofluid, $c_{p,f}$ - the specific heat capacity of fluid, $c_{p,p}$ - the specific heat capacity of particle.

The viscosity of the nanofluid can be estimated with the existing relation

$$\mu_{nf} = \mu_f (1 + \eta \phi), \quad (7)$$

where: μ_{nf} - viscosity of the nanofluid, μ_f - viscosity of the fluid, η - intrinsic viscosity is a measure of a solute's contribution to the viscosity of a solution (Brinkman model $\eta=2.5$) [79].

The equation above is utilized for the calculation of kinematic viscosity, which is applicable to linear viscous fluids with dilution, suspension and spherical particles [80]. A modified Einstein's model for high concentrations of particles up to is as follows:

$$\mu_{nf} = \mu_f (1 - \phi)^{-\eta}, \quad (8)$$

Krieger and Dougherty modified the equation for highly condensed, uniform rigid sphere suspensions.

$$\mu_{nf} = \mu_f \left[1 - \frac{\phi}{\phi_m} \right]^{-\eta \phi_m}, \quad (9)$$

where ϕ_m represents the maximum factor of particle added to the fluid, ranging from 0.495 to 0.54 under steady-state conditions, and it is approximately 0.605 at a high rate of shear [81]. Later, the formula of the dynamic viscosity was modified by [82]

$$\mu_{nf} = \frac{9}{8} \mu_f \left[\frac{\left(\frac{\phi}{\phi_m} \right)^{\frac{1}{3}}}{1 - \left(\frac{\phi}{\phi_m} \right)^{\frac{1}{3}}} \right]. \quad (10)$$

A theory incorporating these effects was developed by [83]. The author considered the contribution of the Brownian motion to the average stress and obtained the following formula for the effective viscosity, accurate to the second-order in concentration [84]:

$$\mu_{nf} = \mu_f (1 + 2.5\phi + 6.2\phi^2). \quad (11)$$

Therefore, the Frankel model of generalized form includes particle radius and the spacing between particles [85].

$$\mu_{nf} = \mu_f \left[1 + 2.5\phi + 4.5 \left(\frac{1}{\left(\frac{H}{dp} \right) \left(2 + \frac{H}{dp} \right) \left(1 + \frac{H}{dp} \right)^2} \right) \right], \quad (12)$$

where: H - nanoparticle diameter, dp - the distance between any two nanoparticles.

The thermal properties of fluid spherical or cylindrical solid particles were studied; moreover, technically and experimentally outstanding prediction formulations on the efficient thermal conductivity of dispersed substances were proposed. A nanoparticle enhances thermal conductivity in a conventional fluid [86].

The expressions of the conventional models of the effective thermal conductivity of a solid/liquid suspension are as follows [87]:

$$k_{nf} = k_f \frac{k_p + 2k_f + 2\phi(k_p - k_f)}{k_p + 2k_f + \phi(k_p - k_f)}, \tag{13}$$

where: k_{nf} - thermal conductivity of nanofluid, k_f - thermal conductivity of fluid, k_p - thermal conductivity of nanoparticle.

The solid line defines the relationship expected by the Hamilton–Crosser prediction equation, in which thermal conductivity is represented as [88]

$$k_{nf} = k_f \frac{k_p + (n-1)k_f + (n-1)\phi(k_p - k_f)}{k_p + (n-1)k_f + \phi(k_p - k_f)}, \tag{14}$$

$$n = \frac{3}{\Psi}, \tag{15}$$

where Ψ is the sphericity ratio between a sphere’s surface area and a particle’s surface area with a volume equal to the parts.

The thermal conductivity aspect is therefore improved by the irregular motion of the nanoparticles suspended and is shown to be the apparent thermal conductivity of the nanofluid [89].

$$k_{nf} = k_f \frac{k_p + 2k_f + 2\phi(k_p - k_f)}{k_p + 2k_f + \phi(k_p - k_f)} + \frac{\rho_p \phi c_p}{2} \sqrt{\frac{k_B T}{3\pi r_c \mu_f}}, \tag{16}$$

where: r_c - the apparent radius of the clusters, Boltzmann constant $k_B = 1.381 \times 10^{-23}$ J/K, T- temperature.

The heat transfer analysis of the direct absorption receiver system (see Fig. 4) under 2D steady state.

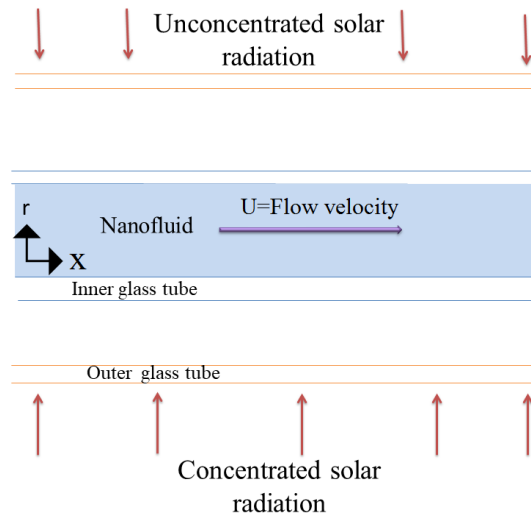


Fig. 4 Section view of the direct absorption receiver system [27]

The nanofluid's thermal conductivity depends on the nanofluid's viscosity and the thermal conductivity of the base liquid and solid particles, as well as the mass, specific heat and volume fraction of the nanoparticles. The heat transfer performance is enhanced by the nanofluid consequent to increasing the properties of the base fluid. The convection heat transfer coefficient is improved due to the increase in volume fraction. The pressure drop increases with the increase in nanofluid density and viscosity [90]. Table 2 shows the effects of various nanofluids on the performance of PTSCs.

Table 2 Effect of various nanofluids on the performance of PTSCs

Ref.	Nanofluid nanoparticle/base fluid)	Volume concentration (%)	Effect on the Performance
[91]	BH-SiO/water TiO ₂ /water	3% 3%	The thermal efficiency is improved by 0.073%, and the coefficient of heat transfer is 138%. The thermal efficiency is improved by 0.073%, and the coefficient of heat transfer is 128%.
[92]	Al ₂ O ₃ /water SiO ₂ /water TiO ₂ /water ZnO/water Al ₂ O ₃ /water Au/ water	(5, 10, 20) % (1, 5, 25) % (1,10,20,35) % (1, 5, 10) % (0.1, 1, 2) % (0.01) %	At low concentrations, only Au, TiO ₂ , ZnO and Al ₂ O ₃ nanofluids pose minimal changes compared with water use; however, increasing nanoparticles concentration does not appear to have any benefit with respect to water. At high temperatures, the viscosity decreases, and the thermal conductivity increases
[93]	Cu/Therminol VP-1 Ag/TherminolVP-1 Al ₂ O ₃ -Therminol VP-1	less than 10%	The thermal efficiency for Ag-TherminolVP-1, Cu -TherminolVP-1 and Al ₂ O ₃ TherminolVP-1 nanofluids improved by 13.9%, 12.5% and 7.2%, respectively. Thermal conductivity increased, the efficiency of exergy improved, and performance of heat transfer improved.
[94]	Graphene/Therminol VP-1, Al/Therminol VP-1	0.02% 0.09%	Graphene has higher solar absorption than nanoparticles in the aluminum particle. DARS can transfer heat at 265.
[95]	Al ₂ O ₃ /Syltherm 800 CuO /Syltherm 800 TiO ₂ / Syltherm 800 Cu/ Syltherm 800	-	Nanofluids boost system efficiency and achieve an increase of up to 1.75% relative to pure thermal oil operations. Moreover, Al ₂ O ₃ and CuO must be used at higher concentrations compared with TiO ₂ and Cu.
[96]	Cu/water	0.02%	Adding of Cu/water significantly improves its absorption characteristics and optical and thermal efficiency and leads to higher outlet temperatures.
[97]	Al ₂ O ₃ / synthetic oil	0.02% 0.04%	The presence of nanoparticles increases the coefficient of heat transfer of the working fluid in the absorber tube.
[98]	Silica/ ethylene glycol Carbon/ ethylene glycol	0.4%	The thermal conductivity increases thermal efficiency by adding solid nanoparticles; for MWCNT and nanosilica, the optimal volume fraction is 0.5% and 0.4%, respectively.

[99]	Al ₂ O ₃ /synthetic oil	0.5%	The thermal performance and overall efficiency improved slightly with the use of Al ₂ O ₃ -synthetic oil. The essential advantage of using nanofluids is reducing the pumping power.
[100]	TiO ₂ /water	2%	The coefficient of convective heat transfer with TiO ₂ /water nanoparticle was increased up to 22.76%, and the maximum efficiency improvement in the PTSC was 8.66% higher than that of the water-based collector.
	OLE-TiO ₂ /water	3%	
	BH-SiO ₂ /water	3%	
[15]	Au /water Al /water Ni/water Ag /water TiO ₂ /water	2%	By adding different concentrations of nanoparticles, particularly for Au-water and Al-water nanofluids in a volume concentration of 2%, the measured values are respectively 2.7 and 2.3 times those for pure water; the critical heat flux is significantly improved.
[101]	CuO/water	0.01% 0.05% 0.1%	Maximum thermal efficiency improvements are achieved by adding CuO nanoparticles to pure water with 0.01%, 0.05% and 0.1% volume fraction; the results were 3.23, 3.6 and 3.82 times those of pure water.
[102]	Fe ₃ O ₄ CuO/Therminol 66	4%	Enhancing the Reynolds number increases the convective heat transfer coefficient. The results show that Fe ₃ O ₄ nanoparticles have great thermal conductivity from CuO particles under the magnetic field.
[103]	Al ₂ O ₃ /synthetic	(1-5)%	The addition of 5% of Al ₂ O ₃ /synthetic nanoparticles improves the efficiency of relative exergy by about 19%. The exergy efficiencies decrease when the wind speeds increase from 5 m/s to 10 m/s.
[104]	CuO / water CuO /oil Al ₂ O ₃ / water Al ₂ O ₃ /oil	1% 3% 5%	At low enthalpy, water performs better than oil as a base fluid. The performance of the base fluid is increased by adding nanoparticle to the oil. As a nanoparticle, CuO has more effect on the energy and energy efficiency of the system than Al ₂ O ₃ because its heat conductivity and density are higher.

7.4.2. Hybrid nanofluid

A new category of nanofluids have the thermophysical properties; they showed improvement and enhancement of the PTSC. Experimental findings allow one to select a suitable model for a given property [105, 106]. The effective properties of the hybrid nanofluids are defined as follows [107, 108]:

$$\rho_{hmf} = \rho_f(1 - \phi_h) + \rho_{p1}\phi_1 + \rho_{p2}\phi_2, \quad (17)$$

where; ρ_{hmf} - hybrid nanofluid density, ρ_{p1} and ρ_{p2} - different types of particle density, ϕ_h - the combined concentration of volume in the hybrid nanofluid of two different types of nanoparticles (ϕ_1 and ϕ_2) as measured.

$$\Phi_h = \Phi_1 + \Phi_2. \quad (18)$$

Heat capacity and viscosity of the hybrid nanofluid can be obtained as follows:

$$c_{p,hnf} = \frac{c_{p,f}(1-\Phi_h) + c_{p,p1}\Phi_1 + c_{p,p2}\Phi_2}{\rho_{hnf}}, \quad (19)$$

$$\mu_{hnf} = \mu_f(1-\Phi_h)^{-\eta}. \quad (20)$$

where: $c_{p,hnf}$ - the specific heat capacity of hybrid nanofluid, μ_{hnf} - viscosity of the hybrid nanofluid.

The hybrid nanofluid thermal conductivity is described in accordance with Maxwell; the following shall be applied:

$$k_{hnf} = \left[\frac{\frac{(\Phi_1 k_{p1} + \Phi_2 k_{p2}) + 2k_f + 2(\Phi_1 k_1 + \Phi_2 k_2) - 2\Phi_h k_f}{\Phi_h}}{\frac{(\Phi_1 k_{p1} + \Phi_2 k_{p2}) + 2k_f - 2(\Phi_1 k_1 + \Phi_2 k_2) - 2\Phi_h k_f}{\Phi_h}} \right]. \quad (21)$$

8. CONCLUSION

The global energy demand is continuously increasing with conventional energy sources depleting. Therefore, fossil fuel resources must be replaced by renewable resources, and the optimal alternative to the traditional energy sources is solar energy due to its inexhaustibility. PTSCs are devices that convert solar radiation into heat. The literature reveals that PTSCs can enhance the heat transfer distribution inside the collectors when they are well designed. Various researchers have studied the PTSC effect and focused their research on modeling, simulation, design and manufacture of the systems in order to determine their performance and the possible improvements that can be made.

The goal is to develop the performance further *via* PTSC modeling and simulation. Modeling studies can show the poor side of the design or possible enhancements in the collector. Therefore, the parametric analyses of the influence are determined with minimum effort and time and low cost in comparison with experimentation. Two main parts which have a considerable effect on the performance of PTSC are the working fluid and the properties of the absorber tube. By using the ANSYS program optimal working parameters are determined in the analysis of PTSCs, which especially heat collector element. Further, it applies to the calculation of a flow rate (laminar or turbulent) and the investigation of heat transfer improvements and modifications using nanofluids and absorber tube configurations.

To improve the performance of PTSCs, different designs have been proposed in the literature. The performance of PTSCs can be improved either by modifying their thermal properties or optical design. The receiver tube affects efficiency under vacuum conditions and coating emittance; it is the major criterion for heat loss. Therefore, optical efficiency is improved by selecting the coating, glass envelope, material and the reflected surface. Heat transfer performance is enhanced by nanofluids consequent to increasing the

properties of the base fluid. A nanofluid improves the thermal and thermodynamic performance of the system. Thermal efficiency depends on the volume fraction of nanoparticles and concentration ratio. The performance of a solar parabolic collector is enhanced by increasing the volume fraction of nanoparticles. The improvements in thermal efficiency relate to low concentrations of nanoparticles. Hybrid nanofluids, a new advanced nanofluid, contain two types of nanoparticles. Hybrid nanofluids enhance the thermal conductivity rate compared with mono nanofluids. Economic viability is considered dependent on capital costs. Moreover, further emphasis should be placed upon the longevity of the material on the nanofluid in the suspension and on the variable costs in the form of maintenance required to replace damages or relieve blockages.

9. FUTURE RECOMMENDATIONS

This review of PTSC literature offered an in-depth insight into research conducted to enhance optical and thermal performance. Few investigations have been performed using nanofluids in compound parabolic-type collectors. The next section highlights the gaps in this area of research for future work to improve the efficiency of PTSCs.

- Coatings for reducing dust particle adhesion and stabilizing temperature operation must be investigated.
- Studies on different shapes of absorber tubes (e.g. elliptical cross section) and their effects on thermal efficiency and distribution of heat flux are recommended.
- Future studies must focus on the methods of avoiding reflector corrosion and increasing of mirror reflectivity property.
- Performance improvements to certain nanoparticles of volume fractions are feasible and can broaden the reach of future research to increase the performance of PTSCs at high volume concentrations.
- Further studies can be conducted with variance in physical geometries to improve the collector the passive convective heat transferring for improving the absorber tube in PTSC.
- The economic effects of the price and expense of nanoparticles of nanofluid preparation synchronizing with the thermal performance enhancement must be investigated to support their efficient application in PTCs.
- Many areas must still be explored by using hybrid nanofluids and mono nanofluids. Alternative combinations of nanoparticles and concentrations of different fluids should still be studied.
- Small-scale nanofluids are still used and tested; large-scale solar power plants must be investigated to implement nanofluids in solar collectors.

REFERENCES

1. Jurasz, J., Canales, F.A., Kies, A., Guezgouz, M., Beluco, A., 2020, *A review on the complementarity of renewable energy sources: Concept, metrics, application and future research directions*, Solar Energy, 195, pp. 703-724.
2. Conrado, L.S., Rodríguez-Pulido, A., Calderón, G., 2017, *Thermal performance of parabolic trough solar collectors*, Renewable and Sustainable Energy Reviews, 67, pp. 1345-1359.
3. Jebasingh, V.K., Herbert, G.J., 2016, *A review of solar parabolic trough collector*, Renewable and Sustainable Energy Reviews, 54, pp. 1085-1091.

4. Yilmaz, S., Riza Ozcalik, H., Dincer, F., 2017, *Modeling and designing of the solar thermal parabolic trough concentrator and its environmental effects*, Environmental Progress & Sustainable Energy, 36(3), pp. 967-974.
5. Sandá, A., Moya, S.L., Valenzuela, L., 2019, *Modelling and simulation tools for direct steam generation in parabolic-trough solar collectors: A review*, Renewable and Sustainable Energy Reviews, 113, 109226.
6. Liu, P., Lv, J., Shan, F., Liu, Z., Liu, W., 2019, *Effects of rib arrangements on the performance of a parabolic trough receiver with ribbed absorber tube*, Applied Thermal Engineering, 156, pp. 1-13.
7. Montes, I.E.P., Benitez, A.M., Chavez, O.M., Herrera, A.E.L., 2014, *Design and construction of a parabolic trough solar collector for process heat production*, Energy Procedia, 57, pp. 2149–2158.
8. Fuqiang, W., Ziming, C., Jianyu, T., Yuan, Y., Yong, S., Linhua, L., 2017, *Progress in concentrated solar power technology with parabolic trough collector system: A comprehensive review*, Renewable and Sustainable Energy Reviews, 79, pp. 1314-1328.
9. Olia, H., Torabi, M., Bahiraei, M., Ahmadi, M.H., Goodarzi, M., Safaei, M.R., 2019, *Application of nanofluids in thermal performance enhancement of parabolic trough solar collector: state-of-the-art*, Applied Sciences, 9(3), 463.
10. Conrado, L.S., Rodriguez-Pulido, A., Calderón, G., 2017, *Thermal performance of parabolic trough solar collectors*, Renewable and Sustainable Energy Reviews, 67, pp. 1345-1359.
11. Fuqiang, W., Jianyu, T., Lanxin, M., Chengchao, W., 2015, *Effects of glass cover on heat flux distribution for tube receiver with parabolic trough collector system*, Energy Conversion and Management, 90, pp. 47-52.
12. Razmmand, F., Mehdipour, R., Mousavi, S.M., 2019, *A numerical investigation on the effect of nanofluids on heat transfer of the solar parabolic trough collectors*, Applied Thermal Engineering, 152, pp. 624-633.
13. Bellos, E., Tzivanidis, C., 2019, *Alternative designs of parabolic trough solar collectors*, Progress in Energy and Combustion Science, 71, pp. 81-117.
14. Akbarzadeh, S., Valipour, M.S., 2018, *Heat transfer enhancement in parabolic trough collectors: A comprehensive review*, Renewable and Sustainable Energy Reviews, 92, pp. 198-218.
15. Mebarek-Oudina, F., Bessaïh, R., 2019, *Numerical simulation of natural convection heat transfer of copper-water nanofluid in a vertical cylindrical annulus with heat sources*, Thermophysics and Aeromechanics, 26(3), pp. 325-334.
16. Mebarek-Oudina, F., 2019, *Convective heat transfer of Titania nanofluids of different base fluids in cylindrical annulus with discrete heat source*, Heat Transfer Asian Research, 48(1), pp. 135-147.
17. Abdelhady, S., Borello, D., Tortora, E., 2014, *Design of a small scale stand-alone solar thermal co-generation plant for an isolated region in Egypt*, Energy conversion and management, 88, pp. 872-882.
18. Price, H., Lupfert, E., Kearney, D., Zarza, E., Cohen, G., Gee, R., Mahoney, R., 2002, *Advances in parabolic trough solar power technology*, Journal of Solar Energy Engineering, 124(2), pp. 109–125.
19. Noor, N., Muneer, S., 2009, *Concentrating Solar Power (CSP) and its prospect in Bangladesh*, 1st International Conference on the Developments in Renewable Energy Technology (ICDRET), IEEE, pp. 1-5.
20. Tian, Y., Zhao, C.Y., 2013, *A review of solar collectors and thermal energy storage in solar thermal applications*, Applied Energy, 104, pp. 538-553.
21. Abdulhamed, A.J., Adam, N.M., Ab-Kadir, M.Z.A., Hairuddin, A.A., 2018, *Review of solar parabolic-trough collector geometrical and thermal analyses, performance, and applications*, Renewable and Sustainable Energy Reviews, 91, pp. 822-831.
22. Behar, O., Khellaf, A., Mohammedi, K., 2015, *A Novel parabolic trough Solar collector model-validation with experimental data and comparison to engineering equation solver (EES)*, Energy Conversion and Management, 106, pp. 268-281.
23. Fernández-García, A., Zarza, E., Valenzuela, L., Pérez, M., 2010, *Parabolic-trough solar collectors and their applications*, Renewable and Sustainable Energy Reviews, 14(7), pp. 1695–1721.
24. Menbari, A., Alemrajabi, A.A., Rezaei, A., 2017, *Experimental investigation of thermal performance for direct absorption solar parabolic trough collector (DASPTC) based on binary nanofluids*, Experimental Thermal Fluid Science, 80, pp. 218-227.
25. Bellos, E., Korres, D., Tzivanidis, C., Antonopoulos, K. A., 2016, *Design, simulation and optimization of a compound parabolic collector*, Sustainable Energy Technologies Assessments, 16, pp. 53–63.
26. Tagle-Salazar, P.D., Nigam, K.D.P., Rivera-Solorio, C.I., 2018, *Heat transfer model for thermal performance analysis of parabolic trough solar collectors using nanofluids*, Renewable energy, 125, pp. 334-343.
27. Zaaoumi, A., Asbik, M., Hafs, H., Bah, A., Alaoui, M., 2021, *Thermal performance simulation analysis of solar field for parabolic trough collectors assigned for ambient conditions in Morocco*, Renewable Energy, 163, pp. 1479-1494.

28. Arias, I., Zarza, E., Valenzuela, L., Pérez-García, M., Romero Ramos, J.A., Escobar, R., 2021, *Modeling and Hourly Time-Scale Characterization of the Main Energy Parameters of Parabolic-Trough Solar Thermal Power Plants Using a Simplified Quasi-Dynamic Model*, *Energies*, 14(1), 221.
29. Mokheimer, E.M.A., Dabwan, Y.N., Habib, M.A., Said, S.A.M., Al-Sulaiman, F.A., 2014, *Techno-economic performance analysis of parabolic trough collector in Dhahran, Saudi Arabia*, *Energy Conversion and Management*, 86, pp. 622-633.
30. Wang, K., Zhang, Z.D., Li, M.J., Min, C.H., 2020, *A coupled optical-thermal-fluid-mechanical analysis of parabolic trough solar receivers using supercritical CO₂ as heat transfer fluid*, *Applied Thermal Engineering*, 183, 116154.
31. Ehtiwesh, I.A., Neto Da Silva, F., Sousa, A.C., 2019, *Deployment of parabolic trough concentrated solar power plants in North Africa—a case study for Libya*, *International Journal of Green Energy*, 16(1), pp. 72-85.
32. Duffie, J.A., Beckman, W.A., Blair, N., 2020, *Solar Engineering of Thermal Processes, Photovoltaics and Wind*, John Wiley & Sons.
33. Agagna, B., Smaili, A., Falcoz, Q., Behar, O., 2018, *Experimental and numerical study of parabolic trough solar collector of MicroSol-R tests platform*, *Experimental Thermal and Fluid Science*, 98, pp. 251-266.
34. Benoit, H., Spreafico, L., Gauthier, D., Flamant, G., 2016, *Review of heat transfer fluids in tube-receivers used in concentrating solar thermal systems: Properties and heat transfer coefficients*, *Renewable and Sustainable Energy Reviews*, 55, pp. 298-315.
35. Cengel, Y., 2014, *Heat and Mass Transfer: Fundamentals and Applications*, McGraw-Hill Higher Education.
36. Mebarek-Oudina, F., 2017, *Numerical modeling of the hydrodynamic stability in vertical annulus with heat source of different lengths*, *Engineering science and technology, an international journal*, 20(4), pp. 1324-1333.
37. Guo, J., Huai, X., 2016, *Multi-parameter optimization design of parabolic trough solar receiver*, *Applied Thermal Engineering*, 98, pp. 73-79.
38. Wu, Z., Li, S., Yuan, G., Lei, D., Wang, Z., 2014, *Three-dimensional numerical study of heat transfer characteristics of parabolic trough receiver*, *Applied Energy*, 113, pp. 902-911.
39. Eck, M., Feldhoff, J.F., Uhlig, R., 2010, *Thermal modelling and simulation of parabolic trough receiver tubes*, *Energy Sustainability*, 43956, pp. 659–666.
40. Patil, R.G., Kale, D.M., Panse, S.V., Joshi, J.B., 2014, *Numerical study of heat loss from a non-evacuated receiver of a solar collector*, *Energy Conversion Management*, 78, pp. 617-626.
41. Patil, R.G., Panse, S.V., Joshi, J.B., 2014, *Optimization of non-evacuated receiver of solar collector having non-uniform temperature distribution for minimum heat loss*, *Energy Conversion and Management*, 85, pp. 70-84.
42. Bellos, E., Tzivanidis, C., 2017, *Parametric investigation of supercritical carbon dioxide utilization in parabolic trough collectors*, *Applied Thermal Engineering*, 127, pp. 736-747.
43. He, Y.L., Xiao, J., Cheng, Z.-D., Tao, Y.-B., 2011, *A MCRT and FVM coupled simulation method for energy conversion process in parabolic trough solar collector*, *Renewable Energy*, 36(3), pp. 976–985.
44. Roldán, M.I., Valenzuela, L., Zarza, E., 2013, *Thermal analysis of solar receiver pipes with superheated steam*, *Applied Energy*, 103, pp. 73-84.
45. Mwesigye, A., Bello-Ochende, T., Meyer, J.P., 2013, *Numerical investigation of entropy generation in a parabolic trough receiver at different concentration ratios*, *Energy*, 53, pp. 114-127.
46. Li, Z.Y., Huang, Z., Tao, W.Q., 2016, *Three-dimensional numerical study on fully-developed mixed laminar convection in parabolic trough solar receiver tube*, *Energy*, 113, pp. 1288-1303.
47. Agagna, B., Smaili, A., Falcoz, Q., 2017, *Coupled simulation method by using MCRT and FVM techniques for performance analysis of a parabolic trough solar collector*, *Energy Procedia*, 141, pp. 34-38.
48. Hachicha, A.A., Rodríguez, I., Capdevila, R., Oliva, A., 2013, *Heat transfer analysis and numerical simulation of a parabolic trough solar collector*, *Applied energy*, 111, pp. 581-592.
49. Selvakumar, N., Barshilia, H. C., 2012, *Review of physical vapor deposited (PVD) spectrally selective coatings for mid-and high-temperature solar thermal applications*, *Solar energy Mater. Solar cells*, 98, pp. 1-23.
50. Hermoso, J.L.N., Sanz, N.M., 2015, *Receiver tube performance depending on cleaning methods*, *Energy Procedia*, 69, pp. 1529-1539.
51. Kennedy, C.E., Terwilliger, K., 2005, *Optical durability of candidate solar reflectors*, *Journal of Solar Energy Engineering*, 127(2), pp. 262-269.
52. Braham, R.J., Harris, A.T., 2009, *Review of major design and scale-up considerations for solar photocatalytic reactors*, *Industrial & Engineering Chemistry Research*, 48(19), pp. 8890-8905.

53. Wirz, M., Petit, J., Haselbacher, A., Steinfeld, A., 2014, *Potential improvements in the optical and thermal efficiencies of parabolic trough concentrators*, Solar Energy, 107, pp. 398-414.
54. Xu, C., Chen, Z., Li, M., Zhang, P., Ji, X., Luo, X., Liu, J., 2014, *Research on the compensation of the end loss effect for parabolic trough solar collectors*, Applied energy, 115, pp. 128-139.
55. Cheng, Z.D., He, Y.L., Wang, K., Du, B.C., Cui, F.Q., 2014, *A detailed parameter study on the comprehensive characteristics and performance of a parabolic trough solar collector system*, Applied thermal engineering, 63(1), pp. 278-289.
56. Li, M., Wang, L.L., 2006, *Investigation of evacuated tube heated by solar trough concentrating system*, Energy Conversion and Management, 47(20), pp. 3591-3601.
57. Bhujangrao, K.H., 2015, *Effect of top glass cover on thermal performance of cylindrical parabolic collector*, International Research Journal of Engineering and Technology, 2(8), 2015.
58. Kasaeian, A., Daviran, S., Azarian, R. D., Rashidi, A., 2015, *Performance evaluation and nanofluid using capability study of a solar parabolic trough collector*, Energy Conversion and Management, 89, pp. 368-375.
59. Bader, R., Pedretti, A., Barbato, M., Steinfeld, A., 2015, *An air-based corrugated cavity-receiver for solar parabolic trough concentrators*, Applied Energy, 138, pp. 337-345.
60. Al-Ansary, H., Zeitoun, O., 2011, *Numerical study of conduction and convection heat losses from a half-insulated air-filled annulus of The receiver of a parabolic trough collector*, Solar Energy, 85(11), pp. 3036-3045.
61. Demagh, Y., Bordja, I., Kabar, Y., Benmoussa, H., 2015, *A design method of an s-curved parabolic trough collector absorber with a three-dimensional heat flux density distribution*, Solar Energy, 122, pp. 873-884.
62. Xiao, X., Zhang, P., Shao, D.D., Li, M., 2014, *Experimental and numerical heat transfer analysis of a V-cavity absorber for linear parabolic trough solar collector*, Energy conversion and management, 86, pp. 49-59.
63. Reddy, K.S., Kumar, K.R., Satyanarayana, G.V., 2008, *Numerical investigation of energy-efficient receiver for solar parabolic trough concentrator*, Heat Transfer Engineering, 29(11), pp. 961-972.
64. Reddy, K.S., Satyanarayana, G.V., 2008, *Numerical study of porous finned receiver for solar parabolic trough concentrator*, Engineering applications of computational fluid mechanics, 2(2), pp. 172-184.
65. Manikandan, G.K., Iniyar, S., Goic, R., 2019, *Enhancing the optical and thermal efficiency of a parabolic trough collector—A review*, Applied energy, 235, pp. 1524-1540.
66. Muñoz, J., Abánades, A., 2011, *Analysis of internal helically finned tubes for parabolic trough design by CFD tools*, Applied Energy, 88(11), pp. 4139-4149.
67. Nadeem, S., Abbas, N., Malik, M.Y., 2020, *Inspection of hybrid based nanofluid flow over a curved surface*, Computer Methods and Programs in Biomedicine, 189, 105193.
68. Ahmadi, M.H., Mirlohi, A., Nazari, M.A., Ghasempour, R., 2018, *A review of thermal conductivity of various nanofluids*, Journal of Molecular Liquids, 265, pp. 181-188.
69. Mebarek-Oudina, F., Aissa, A., Mahanthesh, B., Öztop, H.F., 2020, *Heat transport of magnetized Newtonian nanofluids in an annular space between porous vertical cylinders with discrete heat source*, International Communications in Heat and Mass Transfer, 117, 104737.
70. Verma, S.K., Tiwari, A.K., 2015, *Progress of nanofluid application in solar collectors: a review*, Energy Conversion and Management, 100, pp. 324-346.
71. Al-Oran, O., Lezsovits, F., 2020, *Recent experimental enhancement techniques applied in the receiver part of the parabolic trough collector—A review*, International Review of Applied Sciences and Engineering, 11(3), pp. 209-219.
72. Al-Oran, O., Lezsovits, F., 2020, *Enhance thermal efficiency of parabolic trough collector using Tungsten oxide/Syltherm 800 nanofluid*, Pollack Periodica, 15(2), pp. 187-198.
73. Kakaç, S., Pramuanjaroenkij, A., 2016, *Single-phase and two-phase treatments of convective heat transfer enhancement with nanofluids—A state-of-the-art review*, International journal of thermal sciences, 100, pp. 75-97.
74. Safaei, M.R., Ahmadi, G., Goodarzi, M.S., Safdari Shadloo, M., Goshayeshi, H.R., Dahari, M., 2016, *Heat transfer and pressure drop in fully developed turbulent flows of graphene nanoplatelets-silver/water nanofluids*, Fluids, 1(3), 20.
75. Akbulut, M., Alig, A.R.G., Min, Y., Belman, N., Reynolds, M., Golan, Y., Israelachvili, J., 2007, *Forces between surfaces across nanoparticle solutions: role of size, shape, and concentration*, Langmuir, 23(7), pp. 3961-3969.
76. Potenza, M., Milanese, M., Colangelo, G., de Risi, A., 2017, *Experimental investigation of transparent parabolic trough collector based on gas-phase nanofluid*, Applied Energy, 203, pp. 560-570.

77. Selimefendigil, F., Öztop, H.F., 2014, *MHD mixed convection of nanofluid filled partially heated triangular enclosure with a rotating adiabatic cylinder*, Journal of the Taiwan Institute of Chemical Engineers, 45(5), pp. 2150-2162.
78. Xuan, Y., Roetzel, W., 2000, *Conceptions for heat transfer correlation of nanofluids*, Int. J. Heat Mass Transfer, 43(19), pp. 3701-3707.
79. Vafai, K. ed., 2015. *Handbook of Porous Media*, Crc Press.
80. Umavathi, J.C., Ojjela, O., Vajravelu, K., 2017, *Numerical analysis of natural convective flow and heat transfer of nanofluids in a vertical rectangular duct using darcy-forchheimer-brinkman model*, International Journal of Thermal Sciences, 111, pp. 511-524.
81. Chen, H., Witharana, S., Jin, Y., Kim, C., Ding, Y., 2009, *Predicting thermal conductivity of liquid suspensions of nanoparticles (nanofluids) based on rheology*, Particuology, 7(2), pp. 151-157.
82. Ghadimi, A., Saidur, R., Metselaar, H.S.C., 2011, *A review of nanofluid stability properties and characterization in stationary conditions*, International journal of heat and mass transfer, 54(17-18), pp. 4051-4068.
83. Bashirmezhad, K., Bazri, S., Safaei, M.R., Goodarzi, M., Dahari, M., Mahian, O., Dalkılıç, A.S., Wongwises, S., 2016, *Viscosity of nanofluids: a review of recent experimental studies*, International Communications in Heat and Mass Transfer, 73, pp. 114-123.
84. Sundar, L.S., Singh, M.K., Sousa, A.C., 2013, *Investigation of thermal conductivity and viscosity of Fe₃O₄ nanofluid for heat transfer applications*, International communications in heat and mass transfer, 44, pp. 7-14.
85. Azmi, W.H., Sharma, K.V., Mamat, R., Najafi, G., Mohamad, M.S., 2016, *The enhancement of effective thermal conductivity and effective dynamic viscosity of nanofluids a review*, Renewable and Sustainable Energy Reviews, 53, pp. 1046-1058.
86. Ambreen, T., Kim, M.H., 2020, *Influence of particle size on the effective thermal conductivity of nanofluids: A critical review*, Applied Energy, 264, 114684.
87. Murshed, S.M.S., Leong, K.C., Yang, C., 2005, *Enhanced thermal conductivity of TiO₂-water based nanofluids*, International Journal of thermal sciences, 44(4), pp. 367-373.
88. Abdel Nour, Z., Aissa, A., Mebarek-Oudina, F., Rashad, A.M., Ali, H.M., Sahnoun, M., El Ganaoui, M., 2020, *Magnetohydrodynamic natural convection of hybrid nanofluid in a porous enclosure: numerical analysis of the entropy generation*, Journal of Thermal Analysis and Calorimetry, 141(5), pp. 1981-1992.
89. Özerinç, S., Kakaç, S., Yazıcıoğlu, A.G., 2010, *Enhanced thermal conductivity of nanofluids: a state-of-the-art review*, Microfluidics and Nanofluidics, 8(2), pp. 145-170.
90. Xuan, Y., Li, Q., Hu, W., 2003, *Aggregation structure and thermal conductivity of nanofluids*, AIChE Journal, 49(4), pp. 1038-1043.
91. Mwesigye, A., Huan, Z., Meyer, J.P., 2016, *Thermal performance and entropy generation analysis of a high concentration ratio parabolic trough solar collector with Cu-therminol® VP-1 nanofluid*, Energy Conversion Management, 120, pp. 449-465.
92. Okonkwo, E.C., Essien, E.A., Abid, M., Kavaz, D., Ratlamwala, T.A.H., 2018, *Thermal performance analysis of a parabolic trough collector using water-based green-synthesized nanofluids*, Solar Energy, 170, pp. 658-670.
93. Coccia, G., Di Nicola, G., Colla, L., Fedele, L., Scattolini, M., 2016, *Adoption of nanofluids in low-enthalpy parabolic trough solar collectors: numerical simulation of the yearly yield*, Energy Conversion and Management, 118, pp. 306-319.
94. Mwesigye, A., Meyer, J.P., 2017, *Optimal thermal and thermodynamic performance of a solar parabolic trough receiver with different nanofluids and at different concentration ratios*, Applied Energy, 193, pp. 393-413.
95. Toppin-Hector, A., Singh, H., 2016, *Development of a nano-heat transfer fluid carrying direct absorbing receiver for concentrating solar collectors*, International Journal of Low-Carbon Technologies, 11(2), pp. 199-204.
96. Bellos, E., Tzivanidis, C., 2017, *Parametric analysis and optimization of an organic Rankine cycle with nanofluid based solar parabolic trough collectors*, Renewable Energy, 114, pp. 1376-1393.
97. Ghasemi, S.E., Mehdizadeh Ahangar, G.H., 2014, *Numerical analysis of performance of solar parabolic trough collector with Cu-water nanofluid*, International Journal of Nano Dimension, 5(3), pp. 233-240.
98. Zadeh, P. M., Sokhansefat, T., Kasaeian, A.B., Kowsary, F., Akbarzadeh, A., 2015, *Hybrid optimization algorithm for thermal analysis in a solar parabolic trough collector based on nanofluid*, Energy, 82, pp. 857-864.
99. Kasaeian, A., Daneshzarian, R., Pourfayaz, F., 2017, *Comparative study of different nanofluids applied in a trough collector with glass-glass absorber tube*, Journal of Molecular Liquids, 234, pp. 315-323.

100. Ferraro, V., Settino, J., Cucumo, M. A., Kaliakatsos, D., 2016, *Parabolic trough system operating with nanofluids: comparison with the conventional working fluids and influence on the system performance*, Energy procedia, 101, pp. 782-789.
101. Heyhat, M.M., Valizade, M., Abdolazade, S., Maerefat, M., 2020, *Thermal efficiency enhancement of direct absorption parabolic trough solar collector (DAPTSC) by using nanofluid and metal foam*, Energy, 192, 116662.
102. Malekan, M., Khosravi, A., Syri, S., 2019, *Heat transfer modeling of a parabolic trough solar collector with working fluid of Fe₃O₄ and CuO/Therminol 66 nanofluids under magnetic field*, Applied Thermal Engineering, 163, 114435.
103. Khakrah, H., Shamloo, A., Hannani, S.K., 2018, *Exergy analysis of parabolic trough solar collectors using Al₂O₃/synthetic oil nanofluid*, Solar Energy, 173, pp. 1236-1247.
104. Khan, U., Zaib, A., Mebarek-Oudina, F., 2020, *Mixed convective magneto flow of SiO₂-MoS₂/C₂H₆O₂ hybrid nanoliquids through a vertical stretching/shrinking wedge: Stability analysis*, Arabian Journal for Science and Engineering, 45(11), pp. 9061-9073.
105. Subramani, J., Nagarajan, P.K., Mahian, O., Sathyamurthy, R., 2018, *Efficiency and heat transfer improvements in a parabolic trough solar collector using TiO₂ nanofluids under turbulent flow regime*, Renewable energy, 119, pp. 19-31.
106. Raza, J., Mebarek-Oudina, F., Ram, P., Sharma, S., 2020, *MHD flow of non-Newtonian molybdenum disulfide nanofluid in a converging/diverging channel with Rosseland radiation*, In Defect and Diffusion Forum, 401, pp. 92-106.
107. Ben-Mansour, R., Habib, M.A., 2013, *Use of Nanofluids for improved natural cooling of discretely heated cavities*, Advances in Mechanical Engineering, 5, 383267.
108. Al-Oran, O., Lezsovits, F., Aljawabrah, A., 2020, *Exergy and energy amelioration for parabolic trough collector using mono and hybrid nanofluids*, Journal of Thermal Analysis and Calorimetry, 140, pp. 1579-1596.